Protection and Control of
Modern Power Systems

ORIGINAL RESEARCH

Frequency regularization of a linked wind–diesel system using dual structure fuzzy with ultra-capacitor

Gulshan Sharma[1*] , K. Narayanan[2], T. Adefarati[3] and Sachin Sharma[4]

Abstract

Microgrids (μ-grids) are gaining increased interest around the world for supplying cheap and clean energy. In this paper, a μ-grid comprising a wind turbine generator (WTG) and diesel generator (DG) is considered. It is one of most practical and demanding systems suitable for the present energy crisis in isolated or rural areas. However, wind energy is intermittent in nature while load demand changes frequently. Therefore, a μ-grid can experience large frequency and power fluctuations. The speed governor of the DG tries to minimize the frequency and power deviations in μ-grid though its operation is slow and cannot adequately minimize system deviations. The paper proposes a novel arrangement based on a dual structured fuzzy (DSF) whose structure changes according to the switching limit with a reduced rule base. It has the capability to switch between proportional and integral actions and hence improves the frequency regularization of the μ-grid. The proposed strategy is tested in a μ-grid and the results considering step load alteration, load alteration at different instants of time, nonstop changing load request are compared with some of the well published methods to validate the effectiveness and simplicity of the present design. In addition, it shows that ultra-capacitor establishment in a μ-grid has a positive impact in minimizing system deviations with DSF for the studied cases.

Keywords: Microgrid, Wind generation, Diesel generation, Frequency control, Dual mode fuzzy

1 Introduction

The demand for electricity is ever increasing because of the modernization and mechanical advance of different industries. At present, most electricity need is met through fossil fuel-based power plants. However, as fossil fuels are depleting with increases in fuel price, the electricity requirement may not be met in future by the standard fossil fuel-dependent plants. In this setting, renewable energy sources (RES) present a promising future since they provide the energy via cleaner sources which are not dependent on fossil fuels [1]. Solar power, wind, hydro, biomass, geothermal resources, biofuels and hydrogen

are some of the clean RESs. Among these RESs, wind energy and photovoltaic (PV) have shown widespread adoption because of their environmentally friendly characteristics as well as speedy progression of the design and cost-effective technologies. In addition, they offer some financial benefit as well as social improvement for developing countries [2]. The rising environmental concerns as well as the insufficiency and rising costs of fossil fuels have offered impetus to the integration of RESs in existing power systems. Renewable sources are variable and hence impact the frequency of the system. The idea of a μ-grid in the network with associated and disconnected modes may help improve and control the frequency of the system in rural regions and commercial areas. Power is usually supplied by diesel generators in small and isolated power systems, but wind-based energy generators have also picked up momentum to achieve green energy

*Correspondence: gulshans@uj.ac.za
[1] Department of Electrical Engineering Technology, University of Johannesburg, Johannesburg 2006, South Africa
Full list of author information is available at the end of the article

in isolated or interconnected power systems. Because of sudden changes in either load or wind speed, the system frequency and output power will shift from the standard value resulting in fluctuating frequency and power. This affects stability and the power delivered to customers [3]. A standalone hybrid system comprising of wind turbine generator (WTG), diesel engine generator (DEG), fuel cell and water electrolyzer has been used in [4], in which the effect of the arranged system on load stabilization is considered to ensure quality power supply. The mixture of PV and fuel cell for stand-alone application are shown in [5] aiming to supply power to isolated or rural areas without any interruption. The modeling of joint PV, fuel cell and battery bank system giving power to electric vehicle is studied in [6] the model consists of a PV generator, a proton exchange film fuel cell and a battery bank giving an electric vehicle of 3 kW. In [7], modeling of a PV, wind and fuel cell-based control system is carried out. This outlines the numerical modeling topology and its control organization with a battery bank system. In [8], the modeling and the control of hybrid system are shown. This system comprises wind and PV sources with a battery, and load interfaced through an inverter. The modeling and analysis of a microgrid based renewable system is discussed in [9]. This system contains a wind turbine, a doubly fed induction generator, a PV generator, a fuel cell and a battery bank. Power generation from RES is stochastic in nature and depends upon the climate condition at any time. There will be times when the electrical load does not match the supply. When there is surplus energy is from the RESs, the energy storage devices (ESD) may store the surplus energy for a brief period and release it later to the system when the load requirement is higher. In [10] the authors have presented a hybrid combination of renewable power with flywheel energy storage and compressed energy storage to feed isolated loads and to achieve balance between supply and demand in a stable way through the energy storage devices (ESD). Fluctuation in wind power has a serious impact on the voltage and frequency of the system, and [11] determines that two ESD are more efficient in compensating the fluctuation in wind power and hence improve the standard of system, i.e., voltage and frequency. In [12] the design of a robust controller for frequency regulation of a hybrid system with SMES is shown and it is seen that SMES is quick enough to compensate for wind power fluctuation and to stabilize the system effectively. Better and cheaper ESDs are coming to the market, and thus it is important to explore these new ESDs in isolated power systems. In recent days, the ultra-capacitor (UC) has emerged and is more powerful than other ESDs. UC is a quick acting device which has the capacity to emulate generator rotors to share a sudden power change through its control [13].

Frequency regularization is one of the key features for the efficient and stable operation of interconnected or isolated power systems such as a μ-grid. The applications of a fuzzy logic (FL) strategy have been broadly explored to clarify the issues of real system problems in a practical and broad way. In [14], interval type II fuzzy logic is proposed as secondary control action for a hybrid power system to damp out frequency deviation, though the studies are limited to a multi-area power system. Studies on an isolated μ-grid are presented in [15] using FL adaptive model predictive control. The results verify that FL oriented control is much faster than ordinary model predictive and ordinary PI controls in achieving the targets of the μ-grid. In [16], an optimal FL for a wind integrated system is proposed, whose membership functions are tuned by an optimization technique. However, the FL controller still has a large rule base which may impose limitations on practical implementation. Adaptive polar FL-based control with diminished size of rule base is tried on a multi-area system model in [17] but the studies are limited to a conventional system model. In [18], the online FL tuning approach for system frequency control of multi-area is proposed and executed, but the studies are restricted to a conventional four-area power system to manage the system deviations. In [19] the authors have presented a new design of dual structure fuzzy (DSF) in which the structure of the controller changes according to system error and the output of each mode is tuned by means of FL tuning. This FL mode is designed to operate through a reduced number of rule sets and hence the design can overcome the complexity of traditional FL. However, its application is limited to a system model with a higher capacity of wind power, and no work has been reported to test its application in a μ-grid.

From the literature, it can be seen that μ-grid frequency control is a crucial area of investigation for isolated or rural areas and needs further research and investigation. It is also noted that ESDs can manage small deviations in a shorter time. Additionally, the FL controllers are gaining interest these for power system applications. However, most of the FL controller designs are available for the traditional power system. Research is looking for a combination of FL and optimization techniques only to advance the FL output as present-day applications, while studies lag in finding the design of effective and simpler FL with a reduction in rule base. The reason is that FL design may become complex with large numbers of rules. This can also affect the output of FL for a particular disturbance. The novelties of this paper can be summarized as:

- Demonstrating a µ-grid having a DG and WTG in an interconnected mode to attain continuous power supply considering wind speed variation.
- To achieve a dual structure controller design with fuzzy tuning methodology with reduced rule base such that, at starting when the error is large the controller is activated in one mode while after some time, when the error is small, the controller is shifted to another mode so that steady state value and a low value of the first peak can be achieved.
- The output of DSF is evaluated for load alteration at different instants of time in the µ-grid, for step load change in DG and for continuous load demand variation, while the output is compared with proportional integral (PI) control calculated via the Zeigler-Nichols Method (ZNM) [1] and the recently published D-partition method (DPM) [2].
- It is seen from the investigations that the output of DSF is superior in reaching the original frequency and power of the µ-grid for various case studies. For further improvement, a UC is installed in the µ-grid and the output of DSF is observed for various case studies.

This paper is organized as follows. In Sect. 2, the µ-grid mathematical details and resulting transfer function model are provided. The concept and details of the UC are given in Sect. 3. The model of DSF with reduced rule base is shown in Sect. 4, while the results are analyzed in Sect. 5. The conclusion of the research work is offered in Sect. 6.

2 Modelling of µ-grid

The µ-grid is a blend of WTG and DG, each rated at 150 kW, to realize the required power supply. DG plays a vital part in accomplishing the continuous power supply as WTG depends on the wind condition. Figure 1a show the transfer function diagram of the DG with diesel generator and turbine, and speed representative instruments. The exchange work representation is given as [11]:

$$\Delta P_{GD} = \frac{1}{(1 + sT_{D4})} \Delta P_{GT} \qquad (1)$$

$$\Delta P_{GT} = \left(\frac{K_D(1 + sT_{D1})}{(1 + sT_{D2})(1 + sT_{D3})} \right) \Delta P_G \qquad (2)$$

$$\Delta P_G = \Delta P_{CD} - \left(\frac{1}{R_D} \right) \Delta f \qquad (3)$$

where ΔP_G is the control flag of speed governor (p.u.), ΔP_{GT} is the incremental alteration of the speed governor (p.u.), and ΔP_{CD} is the control input to the governor of
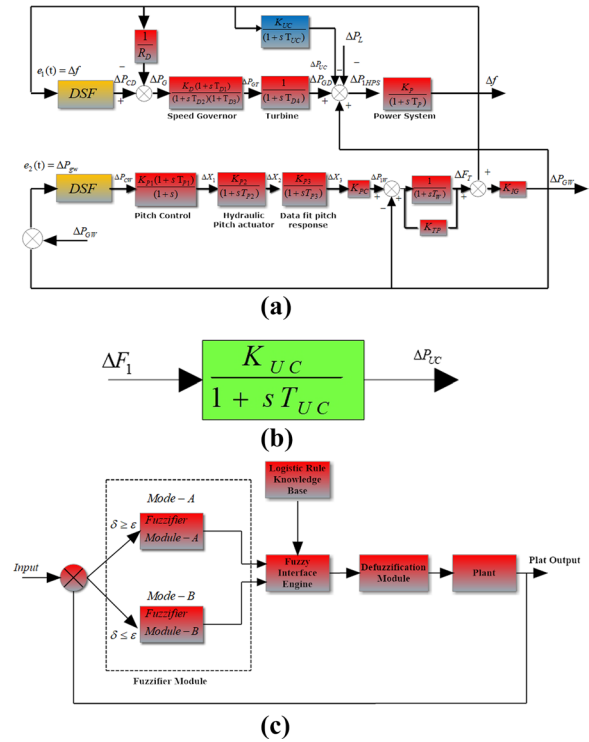
Fig. 1 a Model of µ-grid having DG and WTG, **b** model of UC, **c** schematic of dual structured with fuzzy tuning

the DG unit in (p.u.). ΔF is the frequency modification, K_D is the gain of the governor with T_{D1}, T_{D2}, T_{D3} being the response times of the speed governor. The gain of the turbine is one and T_{D4} is the reaction time of the turbine. R_D is the speed control of the diesel governor. WTG converts wind energy into mechanical and electrical energy. Figure 1a demonstrates the WTG energy conversion process. The fluid coupling system regulates the speed. It compares the turbine and generator frequencies to alter the power output as [11]:

$$\Delta P_{GW} = K_{IG}[\Delta F_T - \Delta f] \qquad (4)$$

K_{IG} is the gain of the fluid coupling with ΔF_T referring to the WTG speed modification. The acceptance generator speed can be written as:

$$\Delta F_T = \left(\frac{1}{1 + sTw} \right) [K_{TP}\Delta F_T - \Delta P_{GW} + K_{PC}\Delta X_3 + \Delta P_{IW}] \qquad (5)$$

where K_{PC} is the gain of edge characteristics, ΔP_{IW} is the input of wind control deviation (in p.u.) and ΔX_3 responds to the data fit pitch (DFP) framework. DFP acts as a lag compensator and its work is to match the gain value of the model. The DFP output can be written as:

$$\Delta X_3 = \Delta X_2 \left[\frac{K_{P3}}{1 + sT_{P3}} \right] \tag{6}$$

In Eq. (6), ΔX_2 is the output of the hydraulic pitch framework (HPF). T_{P3} is the reaction time of DFP with K_{P3} represent the gain of the DFP framework. The work of the hydraulic pitch framework is to control the pitch point of the edges of the wind turbine, and the output of HPF is:

$$\Delta X_2 = \Delta X_1 \left[\frac{K_{P2}}{1 + sT_{P2}} \right] \tag{7}$$

In above equation, ΔX_1 is the pitch controller output with K_{P2} as the gain of the HPF and T_{P2} represents the time constant. The pitch angle system of WTG system needs to be carefully chosen to get the maximum output from the wind turbine. The pitch angle output can be expressed as;

$$\Delta X_1 = \Delta P_{CW} \left[\frac{K_{P1}(1 + sT_{P1})}{1 + s} \right] \tag{8}$$

In above equation, ΔP_{CW} refers to the control flag of the pitch point framework (p.u.), K_{P1} is the gain of the pitch point component with T_{P1} being the reaction time of the pitch point instrument. The total parameters of DG and WTG are recorded in the Reference section. The frequency of μ-grid must be confined to convey quality control. Subsequently the overall control of DG and WTG must coordinate to match the load request. Any change between produced power and load may change the μ-grid frequency and consequently ought to be controlled constantly. Considering the overall power change, the frequency variation of the μ-grid can be expressed as:

$$\Delta f = \Delta P_{IHPS} \left[\frac{K_P}{1 + sT_P} \right] \tag{9}$$

where K_p and T_p represent the gain and time constant of the μ-grid.

3 Modelling of UC

The UC is also known as super-capacitor or double layer electric capacitor and it is one of the most recent developed energy storage devices. It includes two porous electrodes, an ion-exchange layer isolating them, and a potassium hydroxide electrolyte. The electrolyte which is in the liquid form and the porous electrodes in the UC offer a large surface area in comparison to a standard capacitor. In addition, the double layer of slim thickness in a UC provides the specific capacitance. These two factors provides the high capacitance (100–1000 times) in comparison to a standard electrolytic capacitor. The

UC is compact, given its essential thickness, and is able to store a larger amount of energy than standard capacitors. A UC offers a higher ability of power density than a standard battery. It has a higher (specific energy: 1–10 Wh/kg) and (specific power energy: 1–5 kW/kg). It can be charged/discharged millions of times and at a faster rate than a battery or standard capacitors. Hence, a UC is largely maintenance free and offers a lengthy life. All these qualities make it desirable for an updated frequency management in a μ-grid. Using several assumptions, and ignoring nonlinearities, the ultimate outline of a UC can be illustrated through a first-order TF. The frequency deviation of a μ-grid can be expressed as the input to a UC and its TF is given as [13]:

$$\Delta P_{UC}(s) = \left\{ \frac{K_{UC}}{1 + sT_{UC}} \right\} \Delta F(s) \tag{10}$$

where T_{UC} is the time constant and K_{UC} is the select gain of the UC. The selection of K_{UC} is based on state of charge (SOC), and is that at which the UC is charged. Here, K_{UC} is kept at $-7/10$ between 50 and 90% of working SOC of UC. Figure 1b shows the model of the UC.

4 Dual structured fuzzy (DSF)

DSF is an advance method belonging to the category of computational intelligence with fewer control rules. The main benefits of DSF lie in the interpolative nature of fuzzy rules. There is overlapping in the fuzzy antecedents to the control rules which provides the transition amongst the required control actions for various rules. The interpolative quality makes DSF much better than the traditional controllers while it needs fewer rules to perform the given task.

The fuzzy system consists of fuzzy membership functions, an inference engine consisting of if–then rules and is responsible for taking control action as required, and of defuzzification to convert the linguistic values to real values. DSF is better than traditional controllers, e.g. PI, which are good for a particular working situation but become totally unusable if the working condition shifts from the standard conditions. Furthermore, the optimization techniques can improve the outputs to a great extent, but they need more time to calculate the controller gains and hence are not suitable for the μ-grid application. The conventional FLC can be feasible for the operation of a μ-grid, though the complexity in designing the rule base and larger numbers of rules make it unsuitable for a μ-grid. In DSF, there are two fuzzy modules, i.e., Modules A and B. Fuzzy module A acts as fuzzy proportional controller, which will be activated immediately after the disturbance, and will work as long as the error is larger than the switching limit of

Table 1 (a) Rule base for Mode A, (b) rule base for Mode B

If error is	Then K_p is
(a)	
PL	NL
PS	NS
NL	PL
NS	PS

If error is	Then K_i is
(b)	
NB	PB
NM	PM
NS	PS
PS	NS
PM	NM
PB	NB

DSF. If the error is less than or equal to the switching limit of DSF, DSF will work in mode B which is fuzzy integral action and hence it tries to make the steady state error null from the system responses.

Thus, DSF switches from one mode to another automatically and can improve the μ-grid operation. The switching limit of DSF is set as the settling time of system response and 10 s is set as the switching limit of DSF in this study. As DSF operates in two modes, fewer rules are required for each mode and hence its operation becomes faster than traditional controllers. The model of DSF is shown in Fig. 1c. The proposed methodology is isolated into three zones of operation: (a) Assignment of control zone inputs; (b) Improvement of fuzzy rules for fuzzy proportional action (Mode A) and fuzzy integral action (Mode B); (c) Defuzzification of fuzzy values into values as required by the μ-grid. To attain corresponding activity (Kp) by the proposed control plan, the error is dissected into four parts which are positive large (PL), positive small (PS), negative large (NL) and negative small (NS). Triangular membership functions are used because of their simplicity and symmetry. For operation (Ki), the error is divided into negative big (NB), negative medium (NM), negative small (NS), positive small (PS), positive medium (PM) and positive big (PB). Here the triangular membership functions are also chosen for the required action. The rules are listed in Table 1a and b.

After processing in the fuzzification platform, in either mode A or B, the resulting signals are sent to an inference engine platform. This stage is responsible for control actions on the basis of rules formulated. The fuzzy reasoning method adopted in DSF is Mamdani's operation technique. After the inference engine, the final stage

Table 2 Comparison of DSF with ZNM [1] and DPM [2] for step load alteration

| Design	ITAE	IAE
ZNM [1]	48.97	1.121
DPM [2]	5.522	0.312
Dual structure fuzzy	0.2652	0.0202
Dual structure fuzzy + UC	0.2025	0.0012

is defuzzification where the fuzzy set signals are transferred to real values with the help of the well know 'center of gravity' technique in DSF. Mode A operates with only four rules whereas mode B operates with six rules and hence DSF is capable of quickly stabilizing the μ-grid operation in the required time with switching action.

5 Results details and analysis

In this section, DSF is tested as an effective control for the μ-grid control system having DG and WTG. DSF works on the concept that in the event of a sudden load modification in the μ-grid, the μ-grid outputs, i.e., ΔF, P_{WTG} and P_{DG} experience a high first peak and hence DSF will be activated in proportional mode with the fuzzy tuning technique to reduce the magnitude of the first peak. After a few seconds, the system results need to attain the original condition and DSF subsequently works in integral action to return the system back to the steady state value. As DSF works by means of error so a tolerance limit is set for the action to enable the structure to switch from one to another automatically to improve the outputs of the μ-grid. The output (u) accomplished from DSF is associated to DG and WTG.

Initially, the step power request (i.e., 0.01 p.u. load) is connected in the DG of the μ-grid and the performance of DSF is measured by accurate error definition, i.e., the integral of time multiplied by absolute error (ITAE) and integral absolute error (IAE). The output of DSF for the μ-grid for step load modification (0.01 p.u.) is compared with some of the standard and recently published results, i.e., ZNM [1] and DPM [2]. System responses and error values are also compared for different methods.

The ITAE and IAE values are recorded in Table 2, which clearly confirms that the ZNM strategy results in a very high ITAE of 48.97 and IAE of 1.121, while the corresponding ITAE and IAE values with DPM are reduced to 5.522 and 0.312, respectively. With DSF, ITAE and IAE decrease to the lowest values of 0.2652 and 0.0202, respectively. Thus it appears to be the best control for a μ-grid having DG and WTG. System responses during step load modification in DG of the μ-grid are recorded in Fig. 2a–c with different control strategies. The μ-grid with DSF has the least deviations in frequency and power outputs of DG and WTG. The system also goes back to
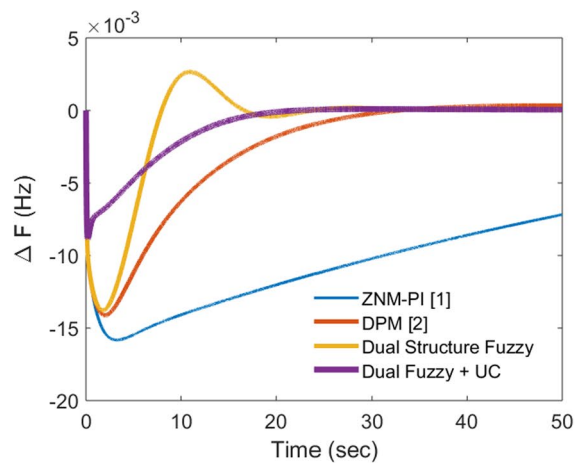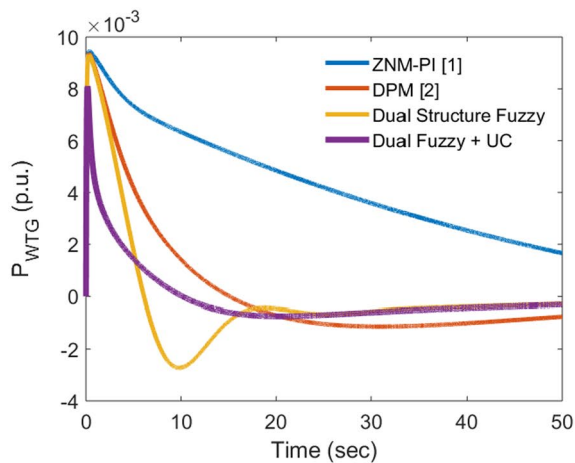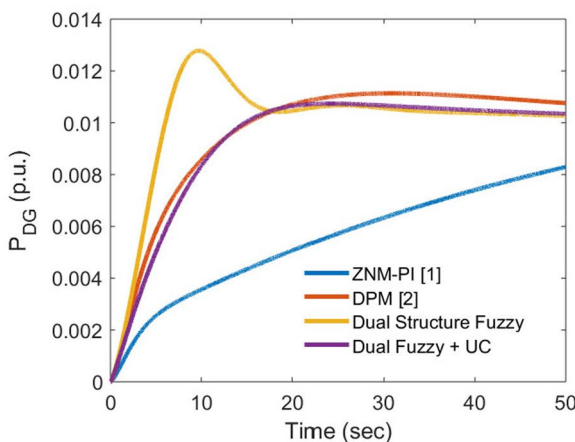
Fig. 2 a–c Output of μ-grid for step load alter in DG

Table 3 Comparison of DSF with ZNM [1] and DPM [2] for load changes at different instants of time

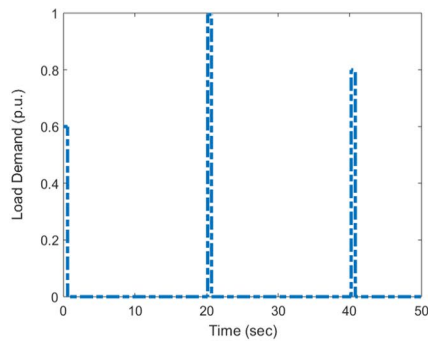| Design	ITAE	IAE
ZNM [1]	228.1	4.745
DPM [2]	300.5	6.065
Dual structure fuzzy	220.1	4.459
Dual structure fuzzy + UC	185.2	2.235

through ZNM experiences the highest overshoot and is not able to realize a consistent state after 50 s.

In further studies, the UC is located in the interlinked DG-WTG in the DG of a μ-grid with frequency deviation as its input while its output is connected to the system at the input to the DG generator. Again, the 0.01 p.u. load is imposed in the DG of the μ-grid and ITAE and IAE are further reduced to 0.2025 and 0.0012, respectively. This indicates that the UC has a positive impact on the μ-grid with DSF. It is seen that when a UC is added the output of DSF under comparable operating conditions advances to a great extent with significant reduction in first peak for all results, as well as the settling of μ-grid deviation becoming smoother with no oscillation. This is due to the UC's ability to quickly release the stored energy to effectively reduce the deviations of the μ-grid.
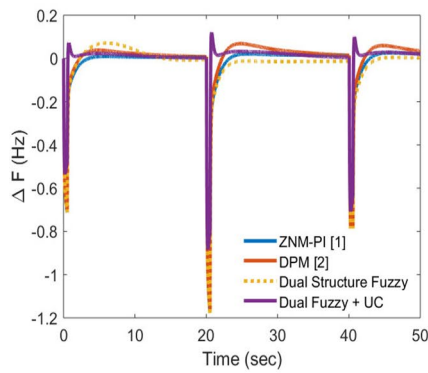
In the next step, the performance of DSF for μ-grid is checked for load variation at specific moments in time. The initial load on the μ-grid is 0.6 p.u.. The load is increased to 1.0 p.u. at 20 s and then decreases to 0.8 p.u. at 40 s. The ITAE and IAE values for this case are shown in Table 3. Error values, i.e., ITAE: 220.1 and IAE: 4.459, are significantly lower with DSF when compared with those obtained via ZNM (ITAE: 228.1 and IAE: 4.745) and DPM (ITAE: 300.5 and IAE: 6.065) methods. In addition, the impact of the UC is also seen in further reducing the errors to ITAE of 185.2 and IAE of 2.235.

The load profile is given in Fig. 3a and various deviation profiles of the μ-grid are given in Fig. 3b–d. The deviation profiles clearly reveal that DSF is effective in reducing the frequency and power deviations of the DG and WTG for the μ-grid during load switching. Further betterment of DSF output is observed when the UC is located in the DG and it is also clearly seen from the Fig. 3.
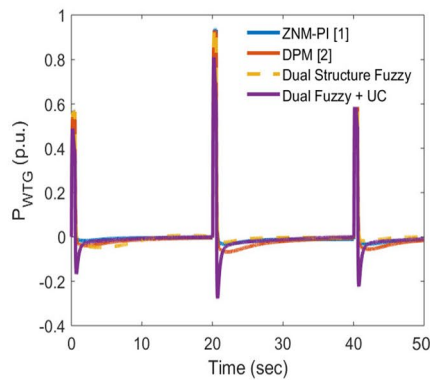
Finally, to check the robust behavior of DSF, persistent load modifications over 50 s at each 10 s are conducted in a μ-grid and the response of DSF is compared with ZNM, DPM and DSF + UC. The load modifications are shown in Fig. 4a and the corresponding μ-grid deviations are illustrated in Fig. 4b–d. The results clearly show that
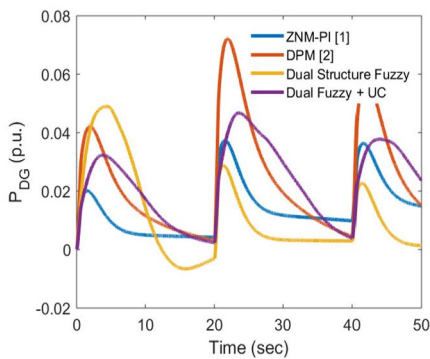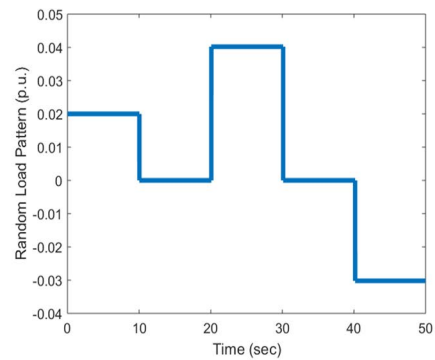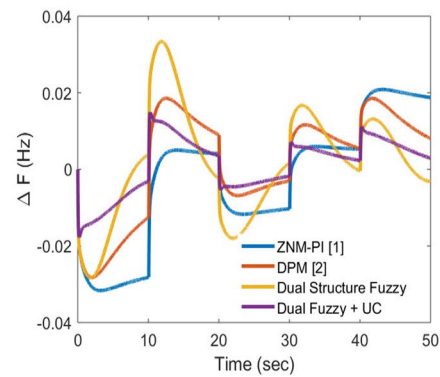
the initial condition quickly. This is not achievable via ZNM or DPM. The response with DPM attempts to go back to original states, while the response obtained

Sharma *et al. Protection and Control of Modern Power Systems*   (2022) 7:12

Page 7 of 9
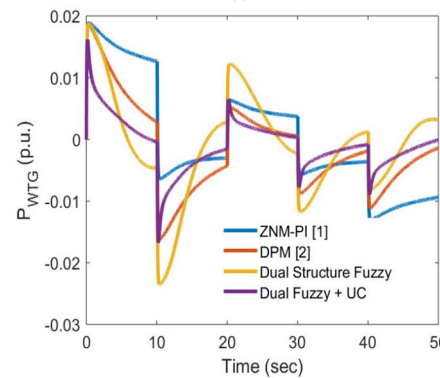

Fig. 3 **a** Load pattern, **b**–**d** output of μ-grid for load variant at different instants of time
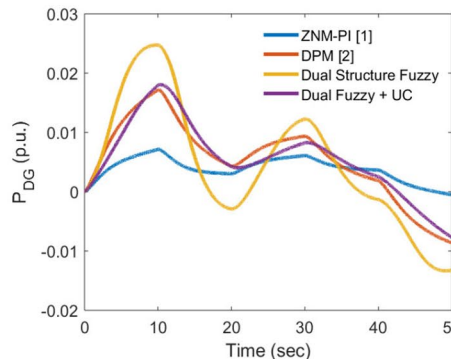
Fig. 4 **a** Continuous load demand, **b**–**d** output of μ-grid for continuous load profile

Sharma *et al. Protection and Control of Modern Power Systems*   (2022) 7:12

Page 8 of 9

the performance of DSF is acceptable when load modifies constantly in the μ-grid when compared with ZNM and DPM. DSF + UC further tracks the continuous load and minimizes frequency and power deviations of DG and WTG in the μ-grid in comparison to ZNM, DPM and DSF. Hence it is verified that the DSF + UC combination is the most successful for various working conditions of the μ-grid.

6 Conclusions

This paper has proposed a new DSF control for minimizing frequency and power deviations of a μ-grid having DG and WTG systems. DSF has the capability to reduce the first peak of overshoot and to eliminate the steady state error from the μ-grid system, as it first operates in fuzzy proportional mode and after some time it automatically changes to integral action according to the switching limit. The new DSF control works on a reduced rule base with the capability of fuzzy and hence its operation is much faster than and superior to other methods for different working conditions of a μ-grid. The μ-grid deviations obtained via DSF are compared with ZNM and DPM strategies for different working conditions. DSF leads to better frequency and power stabilization responses for the μ-grid with shorter settling time and zero unfaltering state when compared to those with ZNM and DPM during step load changes and persistent load modifications at different moments in time. The performance of DSF is also examined in considering error definitions such as ITAE and IAE, and it is seen that ITAE and IAE are reduced significantly with DSF. It is also seen that the same structure of DSF with a UC can further advance the μ-grid results in terms of reduced first peak, faster settling and being oscillation free in all studies, with the lowest ITAE and IAE achieved in comparison to ZNM, DPM. In future, studies can be extended to consider non-linearities of the system and parametric alteration in the μ-grid. They can also look at real-time implementation of μ-grid using DSF.

Appendix: Data [11]

$$K_{P1} = 1.250, \quad K_{P2} = 1.00, \quad K_{P3} = 1.400,$$
$$K_{TP} = 0.0033, \quad K_{IG} = 0.9969$$
$$K_{PC} = 0.0800, \quad T_{P1} = 0.600, \quad T_{P2} = 0.0410,$$
$$T_{P3} = 1.00, \quad T_W = 4.00, \quad R_D = 3.00, \quad T_{D4} = 3.00,$$
$$K_D = 0.333, \quad T_{D1} = 1.00, \quad T_{D2} = 2.00, \quad T_{D3} = 0.025,$$
$$K_p = 120, \quad T_P = 14.4.$$

Author details
[1]Department of Electrical Engineering Technology, University of Johannesburg, Johannesburg 2006, South Africa. [2]Department of Electrical and Electronics Engineering, SASTRA DEEMED UNIVERSITY, Thanjavur, India. [3]Department of Electrical and Electronic Engineering, Federal University Oye Ekiti, Oye Ekiti, Nigeria. [4]Department of Electrical Engineering, Graphic Era (Deemed to be University), Dehradun, India.

References
1. Mallesham, G., Mishra, S., & Jha, A. N. (2011). Ziegler–Nichols based controller parameters tuning for load frequency control in a microgrid. In *International conference on energy, automation and signal (ICEAS)* (pp. 1–8).
2. Veronica, J., Kumar, N. S., & Longatt, F. G. (2020). Design of load frequency control for a microgrid using D-partition method. *International Journal of Emerging Electric Power Systems, 21*(1), 1–11.
3. Gouveia Eduardo, M., & Matos Manuel, A. (2009). Evaluating operational risk in a power system with a large amount of wind power. *Electric Power Systems Research, 79*, 734–739.
4. Senjyu, T., Nakaji, T., Uezato, K., & Funabashi, T. (2005). A hybrid power system using alternative energy facilities in isolated island. *IEEE Transactions on Energy Conversion, 20*(2), 406–414.
5. Rekioua, D., Bensmail, S., & Bettar, N. (2014). Development of hybrid photovoltaic-fuel cell system for stand-alone application. *International Journal of Hydrogen Energy, 39*(3), 1604–1611.
6. Mokrani, Z., Rekioua, D., & Rekioua, T. (2014). Modelling control and power management of hybrid photovoltaic fuel cells with battery bank supplying electric vehicle. *International Journal of Hydrogen Energy, 39*(27), 15178–15187.
7. Mezzai, N., Rekioua, D., Rekioua, T., Mohammedi, A., Idjdarane, K., & Bacha, S. (2014). Modelling of hybrid photovoltaic/wind/fuel cells power system. *International Journal of Hydrogen Energy, 39*(27), 15158–15168.
8. Aissou, S., Rekioua, D., Mezzai, N., Rekioua, T., & Bacha, S. (2015). Modelling and control of hybrid photovoltaic wind power system with battery storage. *Energy Conversion and Management, 89*, 615–625.
9. Tamalouzt, S., Benyahia, N., Rekioua, T., Rekioua, D., & Abdessemed, R. (2016). Performances analysis of WT-DFIG with PV and fuel cell hybrid power sources system associated with hydrogen storage hybrid energy system. *International Journal of Hydrogen Energy, 41*(45), 21006–21021.
10. Wang, L., Lee, D. J., Lee, W. J., & Chen, Z. (2008). Analysis of a novel autonomous marine hybrid power generation/energy storage system with a high-voltage direct current link. *Journal of Power Sources, 185*, 1284–1292.

11. Ganguly, S., Shiva, C. K., & Mukherjee, V. (2018). Frequency stabilization of isolated and grid connected hybrid power system models. *Journal of Energy Storage, 19*, 145–159.

12. Ngamroo, I. (2009). Robust frequency control of wind–diesel hybrid power system using superconducting magnetic energy storage. *International Journal of Emerging Electric Power Systems*. https://doi.org/10.2202/1553-779X.2156.

13. Saha, A., & Saikia, L. C. (2017). Utilization of ultra-capacitor in load frequency control under restructured STPP-thermal power systems using WOA optimized PIDN-FOPD controller. *IET-Generation Transmission and Distribution, 11*(13), 3318–3331.

14. Rawat, S., Jha, B., Panda, M. K., & Kanti, J. (2021). Interval type-2 fuzzy logic control-based frequency control of hybrid power system using DMGS of PI controller. *Applied Sciences, 11*(21), 1–16.

15. Kayalvizhi, S., & Kumar, D. M. V. (2017). Load frequency control of an isolated micro grid using fuzzy adaptive model predictive control. *IEEE Access, 5*, 16241–16251.

16. Abazari, A., Dozein, M. G., & Monsef, H. (2018). An optimal fuzzy-logic based frequency control strategy in a high wind penetrated power system. *Journal of the Franklin Institute, 355*(14), 6262–6285.

17. Chaturvedi, D. K., Umrao, R., & Malik, O. P. (2014). Adaptive polar fuzzy logic based load frequency controller. *International Journal of Electrical Power & Energy System, 66*, 154–159.

18. Khooban, M. H., & Niknam, T. (2015). A new intelligent online fuzzy tuning approach for multi-area load frequency control: Self adaptive modified bat algorithm. *International Journal of Electrical Power & Energy System, 71*, 254–261.

19. Sahoo, S. K., Sharma, G., Panwar, A., & Bansal, R. C. (2019). Frequency regulation of wind integrated power system using dual mode fuzzy. *Energy Procedia, 158*, 6321–6327.